Spin liquid correlations, anisotropic exchange, and symmetry breaking in $Tb_2Ti_2O_7$

Sylvain Petit,[1] Pierre Bonville,[2] Julien Robert,[1] Claudia Decorse,[3] and Isabelle Mirebeau[1]
[1]*CEA, Centre de Saclay, DSM/IRAMIS/Laboratoire Léon Brillouin, F-91191 Gif-sur-Yvette, France*
[2]*CEA, Centre de Saclay, DSM/IRAMIS/Service de Physique de l'Etat Condensé, F-91191 Gif-Sur-Yvette, France*
[3]*ICMMO, Université Paris-Sud, F-91400 Orsay, France*
(Received 27 June 2012; published 5 November 2012)

We have studied the low-energy spin dynamics between 4.6 and 0.07 K in a $Tb_2Ti_2O_7$ single-crystal sample by means of inelastic neutron scattering experiments. The spectra consist in a dual response, with a static and an inelastic contribution, showing striking Q dependencies. We propose an interpretation involving an anisotropic exchange interaction in combination with a breaking of the threefold symmetry at the rare earth site. Simulations of the Q-dependent scattering in the random phase approximation account well for the inelastic response.

DOI: 10.1103/PhysRevB.86.174403 PACS number(s): 75.50.Mm, 61.05.fm, 71.70.Ej, 75.30.Et

Spin liquids now attract considerable attention in modern condensed-matter physics.[1,2] In a classical picture, the localized magnetic moments in such cooperative paramagnets keep fluctuating in a correlated manner, failing to develop long-range order down to very low temperature. From a quantum point of view, a spin liquid ground state can be described by entangled spin wave functions and supports exotic fractionalized excitations also called spinons. Geometrically frustrated magnets are good candidates in the pursuit of such disordered quantum ground states[3] and one of the celebrated examples is the $Tb_2Ti_2O_7$ pyrochlore. It remains in a spin liquid state, with short-range correlated fluctuating moments, down to a temperature as low as 20 mK.[4,5] Since 1999, it has been the subject of many theoretical as well as experimental works, and the origin of its spin liquid ground state is still puzzling.

$Tb_2Ti_2O_7$ belongs to the same family as the $Ho_2Ti_2O_7$ and $Dy_2Ti_2O_7$ spin ices, characterized by an Ising anisotropy along local $\langle 111\rangle$ axes.[6] However, the Tb^{3+} crystal electric field (CEF) with trigonal symmetry[7,8] has a much lower energy gap between the ground-state doublet and the first excited doublet than in spin ices (18 K instead of 200–300 K). It was suggested that, unlike in spin ices, this gap is small enough to allow admixture of excited crystal field states, which produces an effective ferromagnetic contribution that competes with the original antiferromagnetic interactions, and that moves $Tb_2Ti_2O_7$ towards a "quantum spin-ice" regime.[9,10] More recent general descriptions of pyrochlores introduce a minimal Hamiltonian, based on symmetry grounds, for pseudospins 1/2 (the subspace spanned by the ground doublet states $|\psi_\pm\rangle$).[11–13] These models involve an Ising exchange constant J_{zz} responsible for the spin-ice behavior, as well as three "quantum" terms $J_\pm$, $J_{z\pm}$, and $J_{\pm\pm}$ that lift the macroscopic degeneracy of the spin-ice manifold and stabilize a so-called Coulomb phase or so-called U(1) spin liquid phase, describable by an emergent U(1) gauge field. For large quantum couplings, conventional phases are stabilized against the spin liquid. Interestingly, in the particular case of non-Kramers ions (like Tb^{3+}), these phases are characterized by ordering of the $4f$ quadrupoles,[14,15] breaking spontaneously the threefold symmetry of the crystal field.

Recently, we proposed a somehow more phenomenological route to point out the relevance of such a symmetry breaking. Indeed, inelastic neutron scattering experiments have evidenced low-energy spin fluctuations,[8,16,17] which, because of general properties of non-Kramers ions, cannot be explained in the nominal trigonal CEF but can be quite naturally accounted for by assuming a breaking of the threefold symmetry.[18–20] The same conclusion holds in the case of the ordered spin-ice parent compound $Tb_2Sn_2O_7$,[21] where similar, although better defined, strong low-energy fluctuations are also reported.[17,22,23] Experimentally, such a symmetry lowering could be due to a tetragonal distortion precursor to a $T \simeq 0$ Jahn-Teller transition. In $Tb_2Ti_2O_7$, this is supported by thermodynamic measurements,[24,25] by Raman scattering,[26] by some studies of the thermal evolution of the elastic constants,[27–29] as well as by x-ray measurements,[30] but the existence of this distortion is still debated in the literature.[31,32] Recently, motivated by our work,[19] there have been several attempts to determine the characteristics of the low-energy spin dynamics and especially to decide if the fluctuations are quasielastic or inelastic,[32,33] but no consensus was obtained.

In this work, we report high-accuracy and high-resolution inelastic neutron scattering (INS) experiments performed on a $Tb_2Ti_2O_7$ single crystal down to 0.07 K. We unambiguously observe the controversial inelastic excitation. More precisely, we found that the low-energy response is dual; i.e., it is the sum of a rather strong elastic signal and an overdamped inelastic one with striking Q dependencies. By modeling the dynamic susceptibility in the random phase approximation (RPA) and using the anisotropic exchange tensor determined previously,[19] we find that the hypothesis of a breaking of the threefold symmetry reproduces the Q dependence of the inelastic response satisfactorily.

INS experiments have been performed on the triple-axis spectrometer 4F2, installed on the cold neutron source at the LLB-Orphée (Saclay, France) neutron facility.[34] Four $Tb_2Ti_2O_7$ single crystals, of total mass 11 g, synthesized by the floating zone method, were co-aligned in the (hhl) scattering plane. We collected a series of energy scans at various wave vectors along the high-symmetry directions $(hh0)$, $(00l)$, and (hhh) for different temperatures ranging from 0.07 K up to 4 K. We also mapped out the intensity at different constant energy transfers as a function of wave vector in the (hhl) plane. Our data provide compelling evidence for a strong low-energy response, well below the first CEF transition (at about 1.5 meV). The energy resolution $\Delta_0 =$ 0.07 meV [full width at half maximum (FWHM)] allowed us

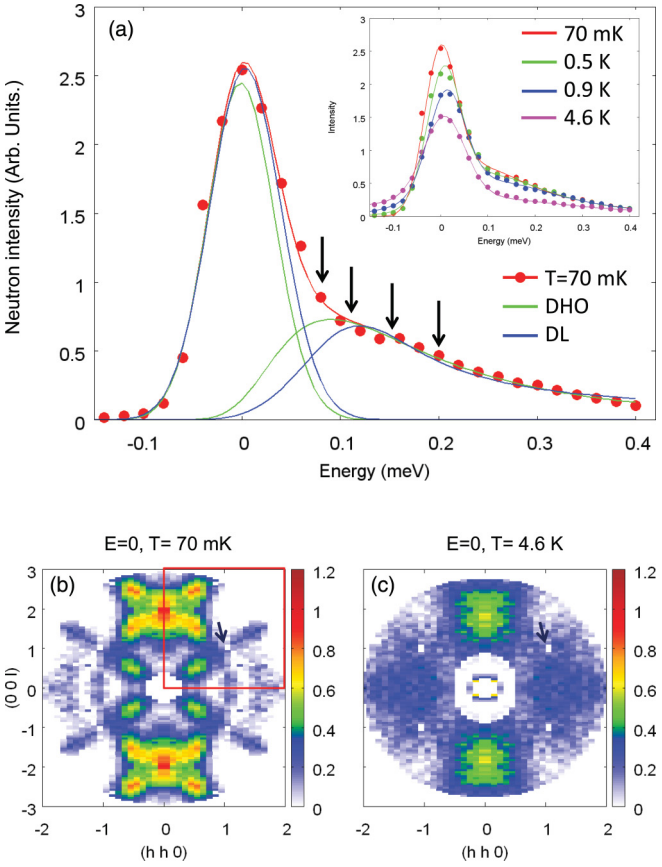

FIG. 1. (Color online) (a) Neutron intensity (normalized to monitor) as a function of energy transfer at $T = 0.07$ K for $Q = (002)$. The data were recorded with a final wave vector $k_f = 1.2$ Å^{-1}, yielding an energy resolution (FWHM) $\Delta_0 = 0.07$ meV. The lines show the elastic and inelastic contributions; the red one shows the total fitted intensity in the case of a damped harmonic oscillator (DHO) for the inelastic contribution (see text). Inset: thermal evolution of the low-energy scattering. (b and c) Elastic magnetic scattering maps taken respectively at 0.07 and 4.6 K. A Q-independent background has been subtracted from the raw data in order to remove the incoherent scattering. It was estimated from the temperature dependence of the total elastic scattering. The color scale is identical for the two temperatures. The red box corresponds to the points actually measured; the remaining has been deduced by symmetry. The pinch point at (111) is marked with an arrow.

to separate an elastic contribution $I_0(Q)$ from a broad inelastic contribution $I_1(Q,\omega)$, with a maximum around 0.15 meV. This is illustrated in Fig. 1, showing the neutron intensity at $Q = (002)$ in the low-energy range $-0.1 \leqslant \omega \leqslant 0.4$ meV. The two contributions are well separated at 0.07 K, where a clear shoulder is observed at finite energy transfer.

This dual response was modeled by $I(Q,\omega) = I_0(Q) + I_1(Q,\omega)$. Note that because of the experimental resolution, $I_0(Q)$ corresponds either to pure static or to slow fluctuations with characteristic energy lower than Δ_0. Like in frustrated ferromagnets, different forms have been used for $I_1(Q,\omega)$: the double Lorentzian (DL) profiles and the damped harmonic oscillator (DHO), with characteristic energy ω_1 and damping [half width at half maximum (HWHM)] Γ_1.[35] After convolution with the experimental resolution function,

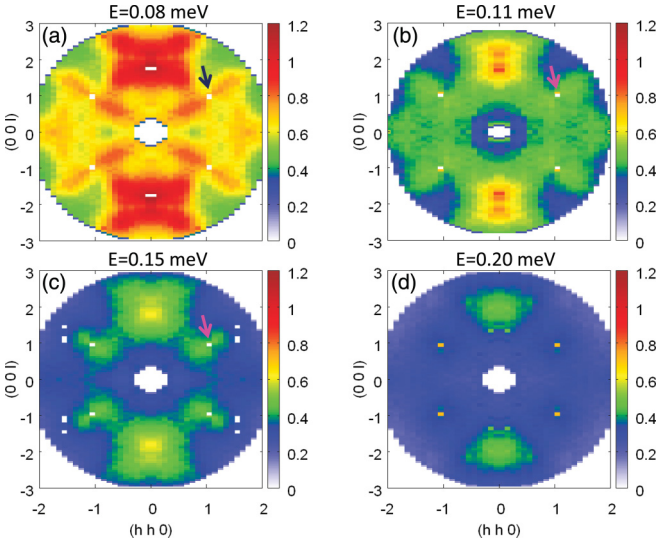

FIG. 2. (Color online) Inelastic scattering maps at 0.07 K for an energy transfer: (a) 0.08, (b) 0.11, (c) 0.15, and (d) 0.20 meV. These energies are indicated by arrows in Fig. 1(a). The pinch point at (111) is also marked with an arrow.

we found that the DHO profile yields the best agreement with the data. Fitting the energy scans recorded along the high-symmetry direction shows almost no change of ω_1 in Q space: $\omega_1 \approx 0.20$ meV, while the damping Γ_1 is large and has the same magnitude: $\Gamma_1 \approx \omega_1$. Maps of $I_0(Q)$ measured at 0.07 and 4.6 K, shown in Fig. 1, reveal a ground state with strongly anisotropic short-range correlations. At 0.07 K, we observe a complex pattern resembling an array of "butterflies" pinned at (002) and, with a smaller intensity, at (220)-type positions. Superimposed on that structure, the map shows lobes centered around (1/2, 1/2, 1/2)-type positions, elongated along the (hhh) directions, and separated by a pinch point at (111).[36] A series of inelastic Q-space maps, taken at 0.07 K at different energy transfers, is shown in Fig. 2. As the energy transfer increases, the pinch point at $Q = (111)$ is progressively "filled" while the intensity at (1/2,1/2,1/2)-type positions decreases. With increasing temperature up to 4.6 K, the intensity of the two signals progressively weakens and the inelastic signal progressively merges into the elastic one. The lobes centered at (1/2,1/2,1/2) persist up to 0.5 K but become barely visible at 4 K, with only weak maxima at (002) and (220)-type positions.

We proceed now to the analysis of the inelastic maps in the (hhl) plane of the reciprocal space. To this end, as mentioned in the introduction, we consider the hypothesis of a breaking of the trigonal symmetry.[18,19] The relevant CEF Hamiltonian reads

$$\mathcal{H}_{\mathrm{CEF}} = \mathcal{H}_{\mathrm{trig}} + \frac{D_Q}{3}\left[2J_x^2 + J_z^2 + \sqrt{2}(J_xJ_z + J_zJ_x)\right], \quad (1)$$

where $\mathcal{H}_{\mathrm{trig}}$ represents the nominal trigonal crystal field[7,8] and the second term a small tetragonal distortion along a cubic [001] axis ($\vec{J}$ is the total angular momentum; for Tb^{3+}, $J = 6$ and the Landé factor is $g_J = 3/2$). The breaking of the threefold symmetry results in a degeneracy lifting and in a mixing of the two states of the ground doublet $|\psi_\pm\rangle$, and stabilizes a CEF singlet state described by the

symmetric wave function $|\psi_s\rangle = \frac{1}{\sqrt{2}}[|\psi_+\rangle + |\psi_-\rangle]$.[18,19] The first excited state is then the antisymmetric combination $|\psi_a\rangle = \frac{1}{\sqrt{2}}[|\psi_+\rangle - |\psi_-\rangle]$, separated from $|\psi_s\rangle$ by a quantity δ proportional to D_Q. In the neutron spectra, this gives rise to an excitation at an energy δ, unveiling the transition from $|\psi_s\rangle$ to $|\psi_a\rangle$. Its intensity is proportional to $\sum_{a=x,y,z} |\langle\psi_s|J^a|\psi_a\rangle|^2$. A straightforward calculation shows that, whereas the general properties of non-Kramers ions impose $\langle\psi_+|\vec{J}|\psi_-\rangle \equiv 0$, the entanglement of $|\psi_\pm\rangle$ yields a sizable $\langle\psi_a|\vec{J}|\psi_s\rangle$ matrix element and thus a large cross section. This accounts for the presence of the low-energy inelastic line in Fig. 1(a). In the absence of entanglement, its intensity would be vanishingly small.[23]

We then introduce the exchange/dipolar Hamiltonian widely accepted for pyrochlores,[7] with an anisotropic exchange tensor $\tilde{\mathcal{J}}_{\rm ex}$ taken to be diagonal in the $(\vec{u},\vec{v},\vec{w})$ frame linked with a Tb-Tb bond along $\vec{w}$.[37] For instance, for the bond along [110], this frame is defined by $\vec{u} = (0,0,1)$, $\vec{v} = \frac{1}{\sqrt{2}}(1,-1,0)$, and $\vec{w} = \frac{1}{\sqrt{2}}(1,1,0)$. The link between this exchange tensor and that employed in Ref. 13 is discussed in the Supplemental Material. For not-too-large antiferromagnetic $\mathcal{J}_{\rm ex}$, depending on the value of the $\tilde{\mathcal{J}}_{\rm ex}/\delta$ ratio, the mean-field ground state of the model is either an ordered spin-ice phase or a singlet yielding no magnetic order, which is quite similar to Bleaney's result for non-Kramers rare earth ions with a singlet CEF ground state.[38]

The set of parameters (D_Q and the exchange tensor components) that stabilizes $|\psi_s\rangle$ as the ground state was determined previously.[19] As described below, we find that within this range the values $D_Q = 0.25$ K, $\mathcal{J}_u = -0.07$ K, $\mathcal{J}_v = -0.2$ K, and $\mathcal{J}_w = -0.1$ K (a negative sign for $\mathcal{J}_i$ means an antiferromagnetic coupling) allow to capture quite well the experimental data. A low-energy inelastic line is expected at $\delta \simeq \omega_1 \simeq 0.22$ meV in the inelastic neutron data. We then calculated the corresponding cross section in the RPA[39–41] as described in the Supplemental Material. A finite width (HWHM) $\Gamma_1 = 0.20$ meV was introduced in the single site susceptibility for the lower transition $|\psi_s\rangle \leftrightarrow |\psi_a\rangle$, according to the DHO fit. The widths of the transitions towards higher crystal field states were set at a smaller value, with no influence on the result.

Figure 3 compares the experimental inelastic scattering [Fig. 3(a)] at 4.6 K for an energy transfer of 0.15 meV with simulations obtained with [Fig. 3(b)] and without [Fig. 3(c)] the tetragonal distortion. The simulated map with distortion is much closer to the experimental data, reproducing the two intense spots at (002) and the rhomb-shaped lesser-intensity scattering centered at (220). The map simulated without distortion, i.e., assuming a degenerate doublet as ground state, is quite different, but it bears resemblance to the diffuse scattering pattern observed at 9 K.[5,39] This points to the fact that the symmetry breaking is probably already present at 4 K, in agreement with the Raman data.[26] At the base temperature (70 mK), the simulated inelastic map [Fig. 3(e)], for an energy transfer of 0.08 meV, also reproduces the structure in Q space reproduced for convenience in Fig. 3(d): the observed butterfly-shaped structures with centers at (002), the high-intensity lines along (111), and the pinch points at (111)-type positions are present. Finally, we examine the influence of

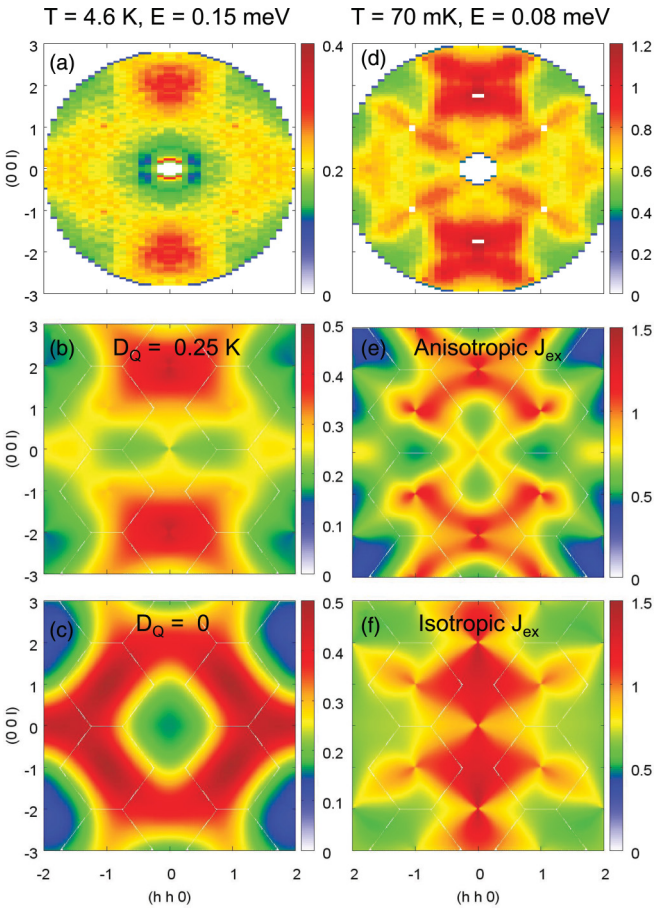

FIG. 3. (Color online) Inelastic scattering maps in $Tb_2Ti_2O_7$. On the left, for $T = 4.6$ K and energy transfer of 0.15 meV: (a) experimental data; (b, c) simulations, using the anisotropic exchange discussed in the text, respectively with and without a tetragonal distortion $D_Q = 0.25$ K. The simulation in (c) has been multiplied by 7000 to obtain the same intensity as in (b). On the right, for $T = 0.07$ K and energy transfer of 0.08 meV: (d) experimental data; (e, f) simulations in the presence of a tetragonal distortion $D_Q = 0.25$ K, with respectively an anisotropic and an isotropic exchange tensor. From these latter maps, it is clear that the Q dependence of the scattering strongly depends on the anisotropy and that it is not reproduced with isotropic exchange.

exchange anisotropy. Figure 3(f) represents a simulation at 0.07 K performed in the same conditions as Fig. 3(e), but for an isotropic exchange constant $\mathcal{J} = -0.04$ K (Ref. 19; note that with this set of parameters, $|\psi_s\rangle$ is also stabilized as the ground state). Its structure does not show the butterfly-shaped pattern observed in the data. Our calculations actually reveal that such a pattern arises only for an anisotropic exchange tensor close to that derived for $Tb_2Ti_2O_7$ ($\mathcal{J}_u = -0.07$ K, $\mathcal{J}_v = -0.2$ K, $\mathcal{J}_w = -0.1$ K).

These RPA simulations thus point to the relevance of the symmetry breaking, leading to a sizable inelastic scattering, while the anisotropy of the exchange coupling does reproduce quite well the Q dependence of the inelastic response. We thus have shown that at this mean-field level the model captures important features relevant to the physics of $Tb_2Ti_2O_7$. It is, however, inadequate to handle other complex features. In particular, the elastic component, namely the structure

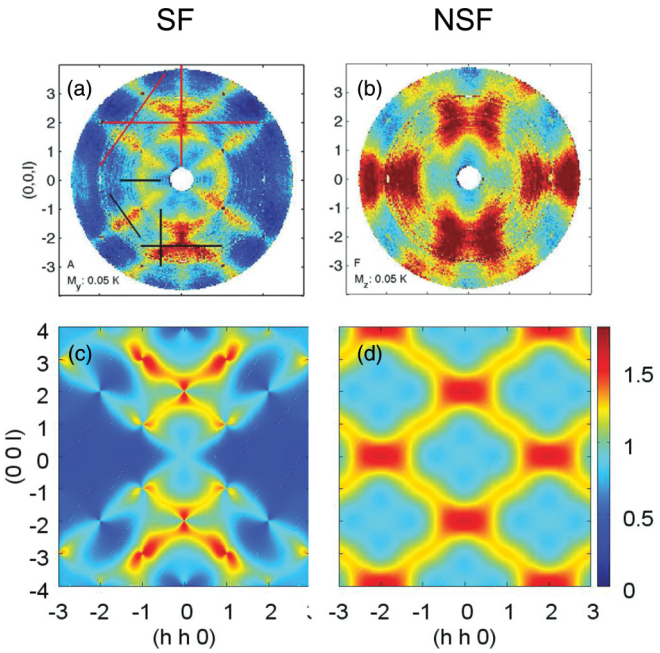

FIG. 4. (Color online) Top: experimental data from Ref. 36: (a) SF and (b) NSF. Bottom: simulated diffuse (c) SF and (d) NSF scattering maps at 0.07 K in $Tb_2Ti_2O_7$.

with lobes at $(1/2,1/2,1/2)$-type positions and in principle given by the Curie term in the expression of the single site susceptibility (see Supplemental Material[34]), is zero since the CEF singlets are nonmagnetic. This is a limitation of the mean-field approach.

To go beyond the present model, different approaches could be suggested. At the level of a single tetrahedron, exact diagonalization of the Tb spin system, currently under way, could possibly capture part of the elastic scattering. Coupling the moments by defects, such as a distribution of distortions, for instance, could yield static correlations[42,43] and the transition seen in susceptibility and specific heat.[25] Other approaches suggest that tunneling processes between different spin-ice configurations also give rise to quasielastic scattering.[11] Finally, we note that recent theoretical models for non-Kramers ions predict new phases characterized by a spontaneous breaking of the threefold symmetry of the crystal field[14,15] as well as an ordering of the $4f$ quadrupoles. Since a coupling between lattice degrees of freedom and such quadrupoles is quite natural, this could provide a new basis for our interpretation.

A paper by Fennell *et al.* appeared[36] after submission of this work. It was performed in different experimental conditions, being an energy-integrated experiment, whereas our measurements are performed with energy analysis of the outcoming neutrons, thus yielding a direct access to the spin fluctuation spectrum. Fennell *et al.* also report on polarized neutron scattering experiments, which allow to distinguish the correlations of spin components along the vertical axis $[1,-1,0]$, in the non-spin-flip (NSF) channel, and correlations of spin components perpendicular to $\vec{Q}$ within the scattering plane in the spin-flip (SF) channel. Figure 4 shows, for both channels, energy-integrated maps at 0.07 K calculated in the framework of our model that capture the experimental data (Figs. 2 A and 2 F of Ref. 36) quite well. The hypothesis of a symmetry breaking and anisotropic exchange are thus compulsory to understand the inelastic response, as we have shown above, but also the diffuse scattering. In conclusion, our INS experiments in $Tb_2Ti_2O_7$ performed down to 0.07 K show unconventional spin dynamics with peculiar features in Q space, such as pinch points and butterfly-shaped patterns in the (hhl) plane, very different from those observed in classical spin ices. We propose an interpretation in terms of a breaking of the threefold symmetry of the crystal field at the Tb^{3+} sites. We present calculations of the inelastic scattering and diffuse cross section of polarized neutrons in the frame of the RPA which support this picture and confirm the anisotropy of the exchange tensor derived previously for $Tb_2Ti_2O_7$.

We would like to acknowledge fruitful discussions with B. Canals, M. Gingras, B. Hennion, P. Holdsworth, and E. Lhotel.

[1] C. Lhuillier and G. Misguich, in *Introduction to Frustrated Magnetism*, edited by C. Lacroix, Ph. Mendels, and F. Mila (Springer, Berlin, 2011).
[2] L. Balents, Nature (London) **464**, 199 (2010).
[3] J. S. Gardner, M. J. P. Gingras, and J. E. Greedan, Rev. Mod. Phys. **82**, 53 (2010).
[4] J. S. Gardner, S. R. Dunsiger, B. D. Gaulin, M. J. P. Gingras, J. E. Greedan, R. F. Kiefl, M. D. Lumsden, W. A. MacFarlane, N. P. Raju, J. E. Sonier, I. Swainson, and Z. Tun, Phys. Rev. Lett. **82**, 1012 (1999).
[5] J. S. Gardner, B. D. Gaulin, A. J. Berlinsky, P. Waldron, S. R. Dunsiger, N. P. Raju, and J. E. Greedan, Phys. Rev. B **64**, 224416 (2001).
[6] H. Cao, A. Gukasov, I. Mirebeau, P. Bonville, C. Decorse, and G. Dhalenne, Phys. Rev. Lett. **103**, 056402 (2009).
[7] M. J. P. Gingras, B. C. den Hertog, M. Faucher, J. S. Gardner, S. R. Dunsiger, L. J. Chang, B. D. Gaulin, N. P. Raju, and J. E. Greedan, Phys. Rev. B **62**, 6496 (2000).
[8] I. Mirebeau, P. Bonville, and M. Hennion, Phys. Rev. B **76**, 184436 (2007).
[9] H. R. Molavian, M. J. P. Gingras, and B. Canals, Phys. Rev. Lett. **98**, 157204 (2007).
[10] B. C. den Hertog and M. J. P. Gingras, Phys. Rev. Lett. **84**, 3430 (2000).
[11] O. Benton, O. Sikora, and N. Shannon, Phys. Rev. B **86**, 075154 (2012).
[12] M. Hermele, M. P. A. Fisher, and L. Balents, Phys. Rev. B **69**, 064404 (2004).
[13] L. Savary and L. Balents, Phys. Rev. Lett. **108**, 037202 (2012).
[14] SungBin Lee, Shigeki Onoda, and Leon Balents, Phys. Rev. B **86**, 104412 (2012).
[15] S. Onoda and Y. Tanaka, Phys. Rev. Lett. **105**, 047201 (2010); Phys. Rev. B **83**, 094411 (2011).
[16] Y. Yasui, M. Kanada, M. Ito, H. Harashina, M. Sato, H. Okumura, K. Kakurai, and H. Kadowaki, J. Phys. Soc. Jpn. **71**, 599 (2002).

[17] K. C. Rule, G. Ehlers, J. S. Gardner, Y. Qiu, E. Moskvin, K. Kiefer, and S. Gerischer, J. Phys.: Condens. Matter **21**, 486005 (2009).
[18] P. Bonville, I. Mirebeau, A. Gukasov, S. Petit, and J. Robert, J. Phys.: Conf. Ser. **32**, 012006 (2011).
[19] P. Bonville, I. Mirebeau, A. Gukasov, S. Petit, and J. Robert, Phys. Rev. B **84**, 184409 (2011).
[20] K. C. Rule and P. Bonville, J. Phys.: Conf. Ser. **145**, 012027 (2009).
[21] I. Mirebeau, A. Apetrei, J. Rodriguez-Carvajal, P. Bonville, A. Forget, D. Colson, V. Glazkov, J. P. Sanchez, O. Isnard, and E. Suard, Phys. Rev. Lett. **94**, 246402 (2005).
[22] K. C. Rule, G. Ehlers, J. R. Stewart, A. L. Cornelius, P. P. Deen, Y. Qiu, C. R. Wiebe, J. A. Janik, H. D. Zhou, D. Antonio, B. W. Woytko, J. P. Ruff, H. A. Dabkowska, B. D. Gaulin, and J. S. Gardner, Phys. Rev. B **76**, 212405 (2007).
[23] S. Petit, P. Bonville, I. Mirebeau, H. Mutka, and J. Robert, Phys. Rev. B **85**, 054428 (2012).
[24] Y. Chapuis, A. Yaouanc, P. Dalmas de Réotier, C. Marin, S. Vanishri, S. H. Curnoe, C. Vaju, and A. Forget, Phys. Rev. B **82**, 100402(R) (2010).
[25] A. Yaouanc, P. Dalmas de Réotier, Y. Chapuis, C. Marin, S. Vanishri, D. Aoki, B. Fak, L.-P. Regnault, C. Buisson, A. Amato, C. Baines, and A. D. Hillier, Phys. Rev. B **84**, 184403 (2011).
[26] T. T. A. Lummen, I. P. Handayani, M. C. Donker, D. Fausti, G. Dhalenne, P. Berthet, A. Revcolevschi, and P. H. M. van Loosdrecht, Phys. Rev. B **77**, 214310 (2008).
[27] L. G. Mamsurova, K. S. Pigal'skii, and K. K. Pukhov, JETP Lett. **43**, 755 (1986).
[28] Y. Nakanishi, T. Kumagai, M. Yoshizawa, K. Matsuhira, S. Takagi, and Z. Hiroi, Phys. Rev. B **83**, 184434 (2011).
[29] V. V. Klekovkina, A. R. Zakirov, B. Z. Malkin, and L. A. Kasatkina, J. Phys.: Conf. Ser. **324**, 012036 (2011).
[30] J. P. C. Ruff, B. D. Gaulin, J. P. Castellan, K. C. Rule, J. P. Clancy, J. Rodriguez, and H. A. Dabkowska, Phys. Rev. Lett. **99**, 237202 (2007).
[31] K. Goto, H. Takatsu, T. Taniguchi, and H. Kadowaki, J. Phys. Soc. Jpn. **81**, 015001 (2012).
[32] B. D. Gaulin, J. S. Gardner, P. A. McClarty, and M. J. P. Gingras, Phys. Rev. B **84**, 140402 (2011).
[33] H. Takatsu, H. Kadowaki, Taku J. Sato, J. W. Lynn, Y. Tabata, T. Yamazaki, and K. Matsuhira, J. Phys.: Condens. Matter **24**, 052201 (2012).
[34] See the Supplemental Material at http://link.aps.org/supplemental/10.1103/PhysRevB.86.174403 for detailed information on the INS experiments.
[35] B. Hennion, M. Hennion, F. Hippert, and A. P. Murani, Phys. Rev. B **28**, 5365(R) (1983).
[36] T. Fennell, M. Kenzelmann, B. Roessli, M. K. Haas, and R. J. Cava, Phys. Rev. Lett. **109**, 017201 (2012).
[37] B. Z. Malkin, T. T. A. Lummen, P. H. M. van Loosdrecht, G. Dhalenne, and A. R. Zakirov, J. Phys.: Condens. Matter **22**, 276003 (2010).
[38] B. Bleaney, Proc. R. Soc. London A **276**, 19 (1963).
[39] Y. J. Kao, M. Enjalran, A. Del Maestro, H. R. Molavian, and M. J. P. Gingras, Phys. Rev. B **68**, 172407 (2003).
[40] J. Jensen and A. R. Mackintosh, *Rare Earth Magnetism* (Clarendon, Oxford, 1991).
[41] A. G. Del Maestro and M. J. P. Gingras, J. Phys.: Condens. Matter **16**, 3339 (2004).
[42] E. Lhotel, C. Paulsen, P. D. deRéotier, A. Yaouanc, C. Marin, and S. Vanishri, Phys. Rev. B **86**, 020410(R) (2012).
[43] S. Legl, C. Krey, S. R. Dunsiger, H. A. Dabkowska, J. A. Rodriguez, G. M. Luke, and C. Pfleiderer, Phys. Rev. Lett. **109**, 047201 (2012).